

Direct numerical simulation of a turbulent curved pipe flow with a 90° bend

Yongmann M. Chung

Zhixin Wang

School of Engineering and Centre for Scientific Computing
University of Warwick
Coventry CV4 7AL, UK
Y.M.Chung@warwick.ac.uk

School of Engineering
University of Warwick
Coventry CV4 7AL, UK
Zhixin.Wang@warwick.ac.uk

ABSTRACT

Direct numerical simulations (DNS) have been performed for a turbulent curved pipe flow going through a 90° bend at Reynolds number $Re_D = 5300$ (or $Re_\tau = 180$). The *swirl switching* phenomenon downstream of the bend is investigated. Mean turbulence statistics in both upstream and downstream of the bend are compared with available DNS and experimental data, and very good agreements have been achieved. Two significant force oscillations in the downstream of the bend are observed: spatial oscillation along the flow direction and temporal oscillation at pipe cross-sections. It is found that the quasi-periodic force oscillation is closely associated with the unsteady motions of Dean vortices. Conditional-averaged flow fields based on positive and negative forces show mirror states of the Dean vortices with one of them being suppressed. It is also observed that the mean flow oscillation is strongly linked with the *swirl switching* phenomenon.

INTRODUCTION

Flows going through curved pipes and channels are very common in industrial applications, *e.g.*, power generation system, water, oil or gas transport pipelines, as well as in human body, *e.g.*, blood flow in vessels and air flow in respiratory (Berger *et al.*, 1983; Kalpakli Vester *et al.*, 2016). The geometry deformation changes the straight pipe/channel flow and introduces flow separation (when curvature ratio is large enough) and secondary motions after the bend. Flow separations and recirculations can cause energy loss and affect the efficiency of fluid transportation. Due to the centrifugal force and local reverse pressure gradient at the pipe bends, a pair of counter-rotating vortices, *i.e.*, Dean vortices (Dean, 1927, 1928), are usually formed downstream of the bend. Such secondary motions result in vibrations of the pipeline systems (Yamano *et al.*, 2011) and cause the fatigue of the pipes (Tunstall *et al.*, 2016). The secondary motions also affect the chemicals or thermal mixing in many applications. Hence, it is very important to understand what, how and why the secondary motion is happening after the bend exit, and also seek for possible methods to control the secondary flow motions where needed. In the present paper, any Reynolds number referred to is defined as $Re_D = U_b D / \nu$, where U_b is the bulk mean velocity in the pipe and D is the pipe diameter. The curvature ratio of the pipe bend is defined as $\gamma = R/R_c$, where R_c is the mean curvature radius at the pipe centreline and $R = D/2$ is the pipe radius.

Turbulent flows in curved pipes have received extensive theoretical and experimental studies since almost a century ago (Dean, 1927). An extensive review of earlier studies is available in Berger *et al.* (1983). Compared with helical (Hüttel & Friedrich, 2001) or infinitely curved (Noorani *et al.*, 2013; Noorani & Schlatter, 2015) pipe flows, flows in 90° bends are of more practical importance and are widely used in industrial applications. Most of the early studies of 90° curved pipe flow focused on the static pressure distributions and head losses in the pipe, and only the mean flow properties were investigated despite the intrinsic unsteady nature of the flow.

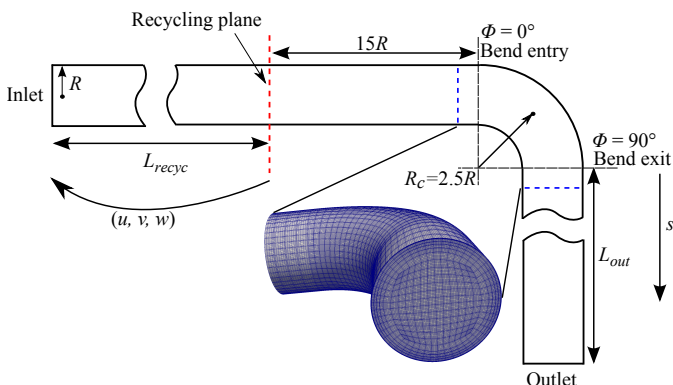


Figure 1. Schematic of the computational domain of a curved pipe with a 90° bend.

Swirl switching

The unsteady behaviour of the Dean vortices after the 90° bend, known as the *swirl switching* phenomenon, has drawn the most attention in the past two decades (Tunstall & Harvey, 1968; Brücker, 1998; Rütten *et al.*, 2001, 2005; Ebara *et al.*, 2010; Ono *et al.*, 2011; Takamura *et al.*, 2012; Sakakibara & Machida, 2012; Kalpakli *et al.*, 2012; Kalpakli & Örlü, 2013; Kalpakli *et al.*, 2013; Hellström *et al.*, 2013; Kalpakli Vester *et al.*, 2015; Carlsson *et al.*, 2015; Tunstall *et al.*, 2016; Noorani & Schlatter, 2016). Tunstall & Harvey (1968) conducted the first detailed experiments to investigate the unsteady behaviour of turbulent flow going through a 90° bend with mitred intersection ($\gamma = \infty$) at $Re_D = 40\,000 - 217\,000$. By injecting talc into the flow after the bend, they observed one dominant swirl that can switch to the mirror state abruptly at a random low frequency. They concluded that the flow going through a 90° bend was essentially bi-stable. The switching frequency of the order of $St = fD/U_b = 0.001$ in their experiments was found to be Reynolds number dependant, *i.e.*, the higher Reynolds number, the larger switching frequency. They also suggested that upstream turbulence and flow separation at the inner corner of the bend are necessary conditions for the switching to occur.

Swirl switching frequency

In addition to the difference in POD modes, one would probably note that the characteristic switching frequency also varies among the previous studies, covering a range from order of 0.001 to order of 0.1. Some studies (Rütten *et al.*, 2001, 2005; Kalpakli & Örlü, 2013; Kalpakli Vester *et al.*, 2015; Noorani & Schlatter, 2016) showed the *swirl switching* phenomenon with a frequency of order of 0.01. Strouhal number of order of 0.1 are often linked with the shear layer instability (Ho & Huerre, 1984) at the inner bend. Tunstall & Harvey (1968) reported very low switching frequencies of order of 0.001. Two dominant frequencies at $St = 0.03$ and 0.12

Table 1. Previous studies related to *swirl switching* in curved pipe flows.

Previous studies	$Re_D \times 10^{-3}$	γ	St
<i>Experimental studies</i>			
Tunstall & Harvey (1968)	40 - 217	∞	0.001 - 0.004
Brücker (1998)	2, 5	0.5	0.03, 0.12
Ebara <i>et al.</i> (2010)	200 - 400	0.5	0.5
Ono <i>et al.</i> (2011)	180, 540	0.33, 0.5	
Takamura <i>et al.</i> (2012)	300 - 1000	0.5	0.5, 1.0
Sakakibara & Machida (2012)	27	0.5	
Kalpakli & Örlü (2013)	34	0.32	0.04, 0.12, 0.18
Kalpakli <i>et al.</i> (2013)	23	0.4	
Hellström <i>et al.</i> (2013)	25	0.5	0.16, 0.33
Kalpakli Vester <i>et al.</i> (2015)	23	0.14, 0.39	0.04, 0.1
<i>LES</i>			
Rütten <i>et al.</i> (2001)	5, 10, 27	0.17, 0.5	0.0055, 0.014, 0.2 - 0.3
Rütten <i>et al.</i> (2005)	5, 10, 27	0.17, 0.5	0.01, 0.2 - 0.3
Carlsson <i>et al.</i> (2015)	34	0.32, 0.5, 0.7, 1.0	0.01, 0.13, 0.5 - 0.6
Tunstall <i>et al.</i> (2016)	108	0.36	0.21, 0.88
<i>DNS</i>			
Noorani & Schlatter (2016)	11.7	0.01, 0.1, 0.3	0.006 - 0.03, 0.06, 0.095
Present	5.3	0.4	0.5, 1.0

were shown in Brücker (1998), where $St = 0.12$ was associated with the oscillation of Dean vortices. Other studies (Hellström *et al.*, 2013; Carlsson *et al.*, 2015; Tunstall *et al.*, 2016) showed much higher switching frequencies. The frequency of the single cell mode was at $St = 0.33$ in Hellström *et al.* (2013). Carlsson *et al.* (2015) investigated the effect of different curvature ratios and found that a frequency at $St \approx 0.5 - 0.6$ becomes more evident when the bend is sharper. They proposed that this frequency is the intrinsic feature of the bend. Takamura *et al.* (2012) measured the velocity fluctuations downstream the bend ($Re_D = 0.3 - 1.0 \times 10^6$), and also showed a characteristic frequency of $St \approx 0.5$ for the circumferential flow motions. This frequency appeared to be Reynolds number independent in their experiments. Tunstall *et al.* (2016) observed a dominant peak at $St = 0.21$ that corresponds to oscillating Dean motions. An even higher frequency peak at $St = 0.88$ was also shown in their LES. Experiment and simulation parameters of previous studies related to *swirl switching* phenomenon is summarised in Table 1.

Present Study

To date, it is well accepted that the turbulent flow after the 90° bend exhibits an unstable bi-modal rather than a bi-stable nature, but the mechanisms underlying the *swirl switching* phenomenon is still not clear. The origin of this intriguing phenomenon also remains unclear. Besides, *swirl switching* appears to exist only in turbulent flow (Tunstall & Harvey, 1968). For a recent review on the progress of experimental and numerical studies of turbulent flows in curved

pipes, one may refer to Kalpakli Vester *et al.* (2016). Despite the importance of turbulent pipe flow with 90° bends in real applications, numerical studies are relatively sparse compared with studies of straight pipes. So far, all of the previous numerical studies performed large-eddy simulations (Rütten *et al.*, 2001, 2005; Carlsson *et al.*, 2015; Tunstall *et al.*, 2016), and direct numerical simulations (DNS) of spatially developing pipe flow with a 90° bend have only started recently (Wang & Chung, 2016; Schlatter *et al.*, 2016). In this study, DNS is performed at $\gamma = 0.4$ and $Re_D = 5300$ to investigate the turbulent flow going upstream, along and downstream a 90° bend.

COMPUTATIONAL DETAILS

Direct Numerical Simulation

The massively parallelised high-order spectral element code, *Nek5000* (Fischer *et al.*, 2008), is used to perform DNS.

$$\frac{\partial u_i}{\partial x_i} = 0, \quad (1)$$

$$\frac{\partial u_i}{\partial t} + \frac{\partial u_i u_j}{\partial x_j} = -\frac{\partial p}{\partial x_i} + \frac{1}{Re_D} \frac{\partial^2 u_i}{\partial x_j \partial x_j}. \quad (2)$$

The massively parallelised high-order spectral element code, *Nek5000* (Fischer *et al.*, 2008), is used. The Reynolds numbers

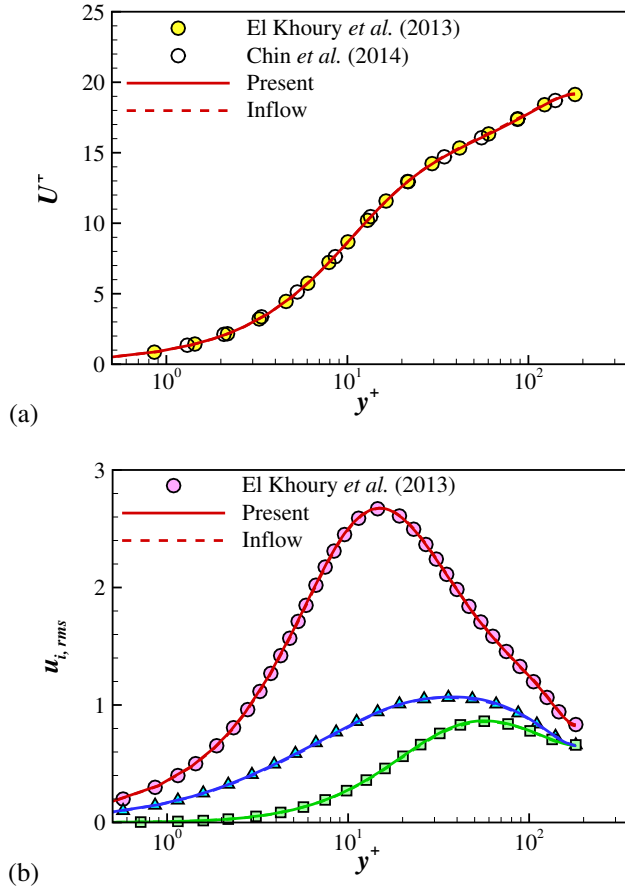


Figure 2. Comparison of (a) mean velocity and (b) velocity fluctuations at $Re_D = 5300$ (or $Re_\tau = 180$). All variables are in wall units. Solid lines represent present straight pipe DNS. Dashed lines represent present curved pipe DNS. Symbols represent DNS data of El-Khoury *et al.* (2013) and Chin *et al.* (2014).

considered are $Re_D = 5300$ (or $Re_\tau = 180$) and $Re_D = 14000$ (or $Re_\tau = 420$). The straight pipe was morphed into a curved pipe with a curvature radius of $R_c = 2.5R$ for $Re_D = 5300$ and $R_c = 3.16R$ for $Re_D = 14000$. A recycling method was implemented to generate a fully developed turbulent inflow condition.

Figure 1 shows the schematic of the computational domain and mesh of the 90° curved pipe. The mesh was generated in a straight pipe first and then morphed into a curved pipe with a curvature ratio of $\gamma = 0.4$. Dirichlet boundary condition was applied at the pipe inlet. A recycling method was implemented to generate a fully-developed turbulent inflow condition. No-slip condition was applied at the pipe wall and no-stress outflow condition was applied at the outlet. The polynomial order for the velocity and pressure spaces was set to be 7 in this study. In the present study, s is defined as the streamwise direction downstream of the 90° bend starting from the bend exit ($s/D = 0$).

First, DNS of turbulent flow in a straight periodic pipe was performed at $Re_D = 5300$ with a pipe length of $30R$. A total number of 49248 elements (about 25 million grid points) were used. The grid resolutions used were similar to those in El-Khoury *et al.* (2013): $\Delta y_{max}^+ \leq 5$ with four grid points below $\Delta y^+ = 1$ and fourteen grid points below $\Delta y^+ = 10$, and $\Delta x_{max}^+ \leq 10$ and $\Delta R\theta_{max}^+ \leq 5$, respectively.

A time step size of $\Delta t^+ \equiv \Delta t u_\tau^2 / \nu \approx 0.1$ (Choi & Moin, 1994)

was used for the straight pipe flow DNS. The turbulence statistics for taking time average were gathered over a time of $t^+ \approx 26000$ after the initial transient stage. All the turbulence statistics were obtained using spatial averaging in both streamwise and circumferential directions as well as time averaging. The mean velocity profile and the root-mean-square (r.m.s.) velocity fluctuations ($u_{i,rms}^+$) are shown in figure 2. DNS data of El-Khoury *et al.* (2013) and Chin *et al.* (2014) are also included for comparison. The present DNS results show an excellent agreement with the available DNS data obtained also using spectral element method.

RESULTS AND DISCUSSION

Inflow Condition

In the present study, a recycling method was implemented in order to generate a fully-developed inflow condition. Recently, DNS of turbulent pipe flows at moderate to high Reynolds numbers have been investigated using large domain sizes up to $30R$ (Chin *et al.*, 2010; El-Khoury *et al.*, 2013). Chin *et al.* (2010) investigated the pipe length effect on the convergence of turbulence statistics in pipe flow with Reynolds number up to $Re_\tau = 500$. They suggested that a domain length of $8\pi R$ would be sufficient for their highest Reynolds number considered. Therefore, the recycling plane in the present study was set to be $L_{recyc} = 25R$ away from the inlet boundary (see figure 1). Velocity components (u , v and w) at the recycling plane were mapped back to the inlet of the pipe. There is a straight pipe section of $15R$ before the flow enters the 90° bend to ensure that the flow at the recycling plane is not affected by the bend. Three outlet lengths of $L_{out} = 25R$, $40R$ and $80R$ were considered to allow the flow to develop. The present study is focused on the unsteady flow motions close to the bend exit.

Turbulence statistics, including mean velocity and velocity fluctuations (see dashed lines in figure 2), obtained from the flow in the upstream recycling section show an excellent agreement with the DNS data in straight pipes (El-Khoury *et al.*, 2013) at the same Reynolds number $Re_D = 5300$. This also shows that the turbulent flow going into the pipe bend is fully developed.

Mean Flow Field

As shown in Figure 3(a), after the bend, high-speed fluid is forced to move towards the outer (concave) side of the pipe due to the centrifugal forces while low-speed fluid is moved to the inner (convex) side of the pipe. The flow separates before leaving the bend exit in the convex side, and a small recirculating flow region is observed. The time-averaged in-plane motions of a cross-section $0.67D$ downstream the bend exit show a pair of counter-rotating vortex rolls (Figure 3(b)), *i.e.*, the so-called Dean vortices. Figure 3(c) shows the instantaneous motions of the Dean vortices at three time instants. These Dean vortices change their strengths and positions in the instantaneous flow field. The flow separates at the inner side before leaving the bend exit, and a flow recirculation region is formed (figure ??(a)). Two flow separation regions are clearly observed from the time-averaged streamwise velocity, one at the inner corner of the bend and the other at the outer corner of the bend.

Downstream streamwise velocity profile along the axis of symmetry at $s/D = 1$ (not shown here) agrees well with the experimental data of Brücker (1998), taking into account the small differences of Re_D and γ . The flow gradually recovers as it moves further downstream the bend. It can be seen that the pipe flow is still not fully recovered even after $10D$ downstream of the bend at this relatively low Reynolds number $Re_D = 5300$.

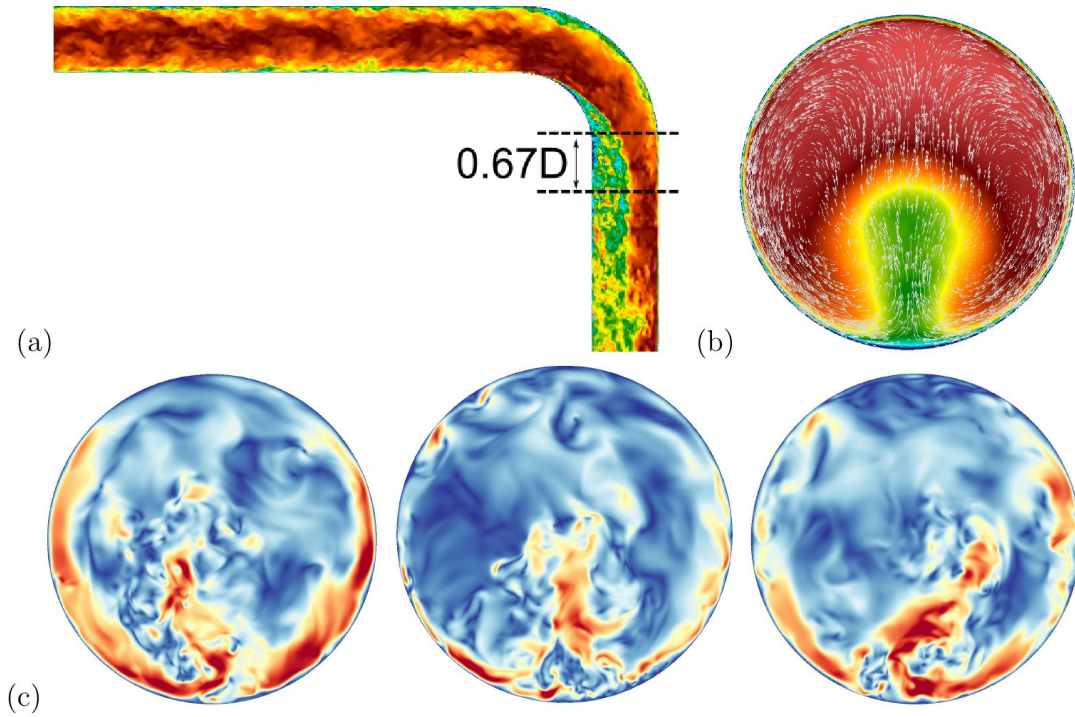


Figure 3. (a) Instantaneous streamwise velocity, (b) time-averaged, and (c) instantaneous in-plane velocity.

Oscillatory Flow Motions

It has been observed in the previous studies that the Dean vortices change their strengths and sizes in the instantaneous flow fields. The two vortices take turns to dominate each other in terms of size and strength, and the unsteady motions of Dean vortices are often referred to as the *swirl switching* phenomenon.

The pressure force exerting on the pipe wall is calculated. Figure 4 shows the oscillation of the horizontal component f of total force on the pipe wall. In order to investigate the flow dynamics associated with the horizontal force fluctuation, conditional averaging of the instantaneous flow fields at $s/D = 1$ was performed. Conditional averaging were performed for $|f| > 1.5\sigma$, where σ is the rms value of the horizontal force oscillation, f_{rms} . Positive and negative force events are denoted as f^+ and f^- . The reason for choosing this downstream location is that f_{rms} has its maximum at $s/D = 1$. Also, no *swirl switching* was observed very close to the bend exit ($s/D \leq 0.2$) (Brücker, 1998; Kalpakli *et al.*, 2013). The conditionally-averaged flow fields are shown in figure ?? together with the time-averaged flow fields. The Dean vortices are clearly seen in the time-averaged flow field in figures ??(a-c). It is found that the wall force fluctuation is closely associated with the oscillation of the Dean vortices. For example, in the positive force (f^+) events in figures ??(d-f), the clockwise vortex on the left side of the pipe is dominant, while the anticlockwise vortex on the right side is significantly suppressed. The vortex on the left side is stronger in strength as well as larger in size than the right side one. As a result, the plane of symmetry is tilted in the clockwise direction. The opposite trend, that is, a stronger clockwise vortex on the right side with a weaker anticlockwise vortex on the left side, is observed in the negative force (f^-) events in figures ??(g-i). It is interesting to note that these in-plane flow motions are similar to those reconstructed from the most energetic POD modes in previous studies (Kalpakli *et al.*, 2012, 2013; Kalpakli & Örlü, 2013; Hellström *et al.*, 2013; Carlsson *et al.*, 2015; Kalpakli Vester *et al.*, 2015; Tunstall *et al.*, 2016; Noorani & Schlatter, 2016).

It is also observed that the mean flow oscillation is strongly linked with the *swirl switching* phenomenon (figures 5(d) and (g)). To study the relationship between the mass flow imbalance and force fluctuations, streamwise velocity is integrated on the left and right sides of the pipe, respectively. When the pipe endures, *e.g.*, positive horizontal force f^+ , the mass flow on the left side of the pipe is larger than on the right side, and vice versa. In other words, the side with stronger vortex also has higher mass flow rate. The horizontal force fluctuation is associated with a frequency of $St \approx 0.5$, with occasional high frequency oscillation at $St \approx 1.0$. The mass flow fluctuation also shows a dominant frequency at $St \approx 0.5$. A similar frequency associated with the flow oscillations was also reported in earlier experimental ($St \approx 0.5$) (Takamura *et al.*, 2012; Ebara *et al.*, 2010) and numerical ($St = 0.5 - -0.6$) (Carlsson *et al.*, 2015) studies. The frequency of the pressure fluctuations (Ebara *et al.*, 2010) and circumferential velocity fluctuations (Takamura *et al.*, 2012) appears to be Reynolds number independent in the measurements. The LES study (Carlsson *et al.*, 2015) suggested that this switching frequency is an intrinsic feature of the bend as it becomes more dominant when the bend is sharper. One should also note that in those studies, similar to the present study, the bend considered were relatively sharp ($\gamma \geq 0.32$).

CONCLUSIONS

In this study, the *swirl switching* phenomenon in a 90° curved pipe is investigated by DNS. The Reynolds number considered is $Re_D = 5300$ and the curvature ratio of the bend is $\gamma = 0.4$. A recycling turbulent inflow boundary condition was implemented and the turbulence statistics from the recycling region show an excellent agreement with DNS data in the straight pipe flow. Mean flow field in the downstream of the bend compares well with available experimental data at similar Reynolds number and bend curvature. The unsteady motions of Dean vortices were studied through the pressure and force oscillations on the pipe wall. The force considered in this study is the component perpendicular to the symmetry plane of the geometry. Two significant force oscillations are ob-

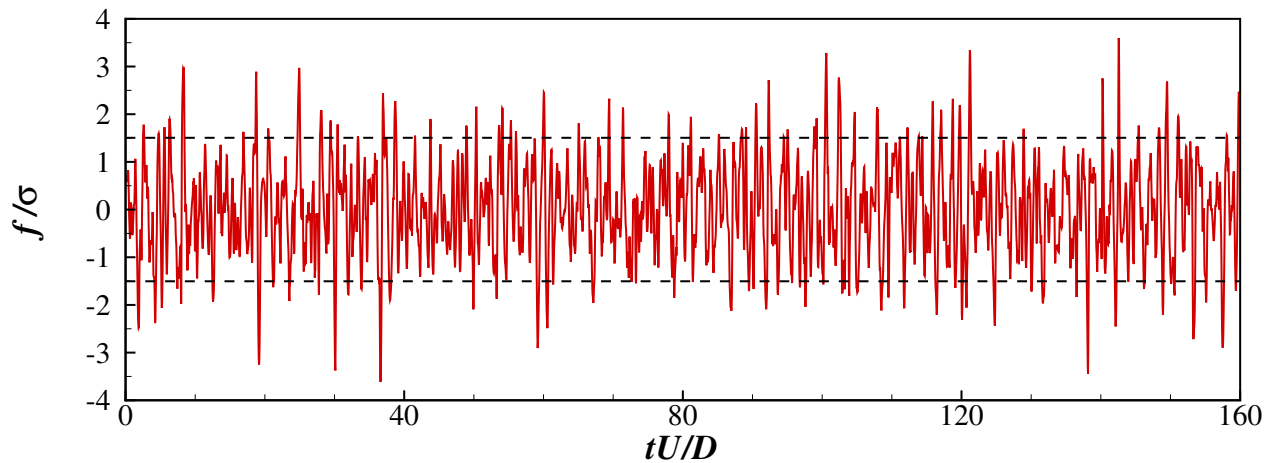


Figure 4. Horizontal force fluctuation at $s/D = 1$. Dashed lines indicate $f/\sigma = \pm 1.5$. σ is the r.m.s. value of the horizontal force fluctuation.

served: spatial oscillation that travels with the flow to the further downstream after the bend, and temporal oscillation at certain pipe cross-sections. The force oscillation is found to be closely associated with the unsteady motions of the Dean vortices, *i.e.*, *swirl switching* phenomenon. Conditional-averaged flow fields for positive and negative force events show mirror states of the Dean vortices, that is vortex on one side of the pipe is dominant while the other is suppressed. The force oscillation associated with the vortex motions is explained through the wall pressure distribution. The oscillation of the mean flow is observed to strongly correlate with the force oscillation (or vortex motions). The side with stronger vortex has higher mass flow rate than the other side. Both force and mean flow fluctuations show a frequency at $St \approx 0.5$.

REFERENCES

- Berger, S. A., Talbot, L. & Yao, L. S. 1983 Flow in curved pipes. *Annual Review of Fluid Mechanics* **15**, 461–512.
- Brücker, Ch. 1998 A time-recording DPIV-study of the swirl switching effect in a 90° bend flow. In *8th International Symposium on Flow Visualisation*, pp. 171.1–171.6. 1-4 September, Sorrento, Italy.
- Carlsson, C., Alenius, E. & Fuchs, L. 2015 Swirl switching in turbulent flow through 90° pipe bends. *Physics of Fluids* **27**, 085112.
- Chin, C., Monty, J. P. & Ooi, A. 2014 Reynolds number effects in DNS of pipe flow and comparison with channels and boundary layers. *International Journal of Heat and Fluid Flow* **45**, 33–40.
- Chin, C., Ooi, A. S. H., Marusic, I. & Blackburn, H. M. 2010 The influence of pipe length on turbulence statistics computed from direct numerical simulation data. *Physics of Fluids* **22** (11), 115107.
- Choi, H. & Moin, P. 1994 Effects of the computational time step on numerical solutions of turbulent flow. *Journal of Computational Physics* **113** (1), 1–4.
- Dean, W. R. 1927 Note on the motion of fluid in a curved pipe. *Philosophical Magazine* **4** (20), 208–223.
- Dean, W. R. 1928 The stream-line motion of fluid in a curved pipe. *Philosophical Magazine* **5** (30), 673–695.
- Ebara, S., Aoya, Y., Sato, T., Hashizume, H., Kazuhisa, Y., Aizawa, K. & Yamano, H. 2010 Pressure fluctuation characteristics of complex turbulent flow in a single elbow with small curvature radius for a Sodium-cooled fast reactor. *ASME: Journal of Fluids Engineering* **132** (11), 111102.
- El-Khoury, G. K., Schlatter, P., Noorani, A., Fischer, P. F., Brethouwer, G. & Johansson, A. V. 2013 Direct numerical simulation of turbulent pipe flow at moderately high Reynolds numbers. *Flow, Turbulence and Combustion* **91** (3), 475–495.
- Fischer, P. F., Lottes, J. W. & Kerkemeier, S. G. 2008 nek5000 Web page. <http://nek5000.mcs.anl.gov>.
- Hellström, L. H. O., Zlatinov, M. B., Cao, G. & Smits, A. J. 2013 Turbulent pipe flow downstream of a 90° bend. *Journal of Fluid Mechanics* **735**, R7.
- Ho, C.-M. & Huerre, P. 1984 Perturbed free shear layers. *Annual Review of Fluid Mechanics* **16**, 365–424.
- Hüttl, T. J. & Friedrich, R. 2001 Direct numerical simulation of turbulent flows in curved and helically coiled pipes. *Computers and Fluids* **30** (5), 591–605.
- Kalpakli, A. & Örlü, R. 2013 Turbulent pipe flow downstream a 90° pipe bend with and without superimposed swirl. *International Journal of Heat and Fluid Flow* **41**, 103–111.
- Kalpakli, A., Örlü, R. & Alfredsson, P. H. 2012 Dean vortices in turbulent flows: rocking or rolling? *Journal of Visualization* **15** (1), 37–38.
- Kalpakli, A., Örlü, R. & Alfredsson, P. H. 2013 Vortical patterns in turbulent flow downstream a 90° curved pipe at high Womersley numbers. *International Journal of Heat and Fluid Flow* **44**, 692–699.
- Kalpakli Vester, A., Örlü, R. & Alfredsson, P. H. 2015 POD analysis of the turbulent flow downstream a mild and sharp bend. *Experiments in Fluids* **56** (3), 57.
- Kalpakli Vester, A., Örlü, R. & Alfredsson, P. H. 2016 Turbulent flows in curved pipes: recent advances in experiments and simulations. *Applied Mechanics Review* **68** (5), 050802.
- Noorani, A., El Khoury, G. K. & Schlatter, P. 2013 Evolution of turbulence characteristics from straight to curved pipes. *International Journal of Heat and Fluid Flow* **41**, 16–26.
- Noorani, A. & Schlatter, P. 2015 Evidence of sublamina drag naturally occurring in a curved pipe. *Physics of Fluids* **27** (3), 035105.
- Noorani, A. & Schlatter, P. 2016 Swirl-switching phenomenon in turbulent flow through toroidal pipes. *International Journal of Heat and Fluid Flow* **61**, 108–116.
- Ono, A., Kimura, N., Kamide, H. & Tobita, A. 2011 Influence of elbow curvature on flow structure at elbow outlet under high Reynolds number condition. *Nuclear Engineering and Design* **241** (11), 4409–4419.
- Rütten, F., Meinke, M. & Schröder, W. 2001 Large-eddy simulations of 90° pipe bend flows. *Journal of Turbulence* **2** (3), 1–14.

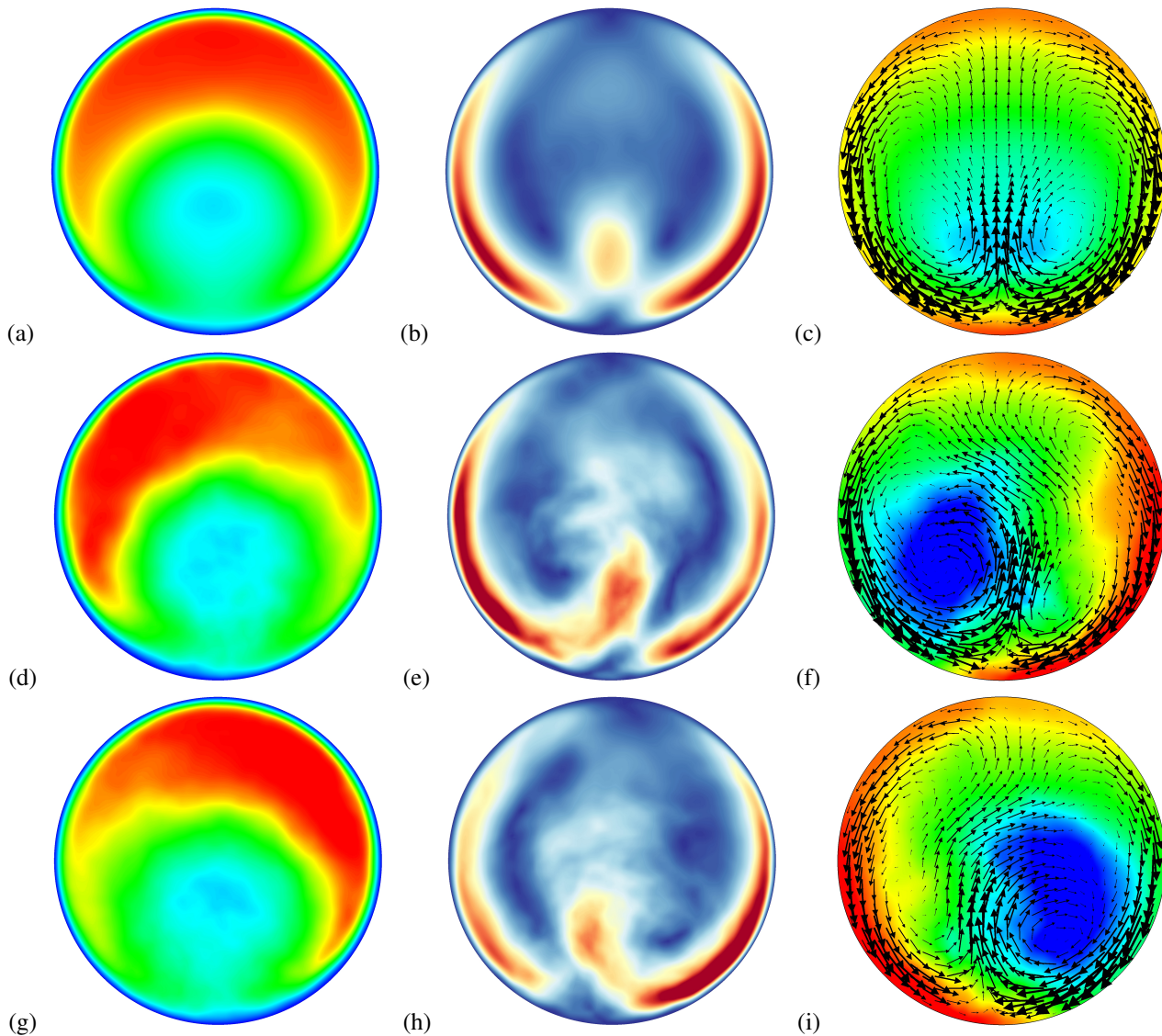


Figure 5. Streamwise velocity (a, d, g), in-plane velocity magnitude (b, e, h) and in-plane velocity vectors and pressure (c, f, i) at $s/D = 1$. (a-c) Time-averaged flow fields. (d-f) Conditional-averaged flow fields for positive force (f^+), and (g-i) for negative force (f^-) events. Same contour levels are used for the same quantity.

Rütten, F., Schröder, W. & Meinke, M. 2005 Large-eddy simulations of low frequency oscillations of the Dean vortices in turbulent pipe bend flows. *Physics of Fluids* **17** (3), 035107.

Sakakibara, J. & Machida, N. 2012 Measurement of turbulent flow upstream and downstream of a circular pipe bend. *Physics of Fluids* **24** (4), 041702.

Schlatter, P., Hufnagel, L., Canton, J., Örlü, R., Marin, O. & Merzari, E. 2016 Unravelling the mechanism behind Swirl-Switching in turbulent bent pipes. In *69th Annual Meeting of the APS Division of Fluid Dynamics*. 20-22 November, Portland, USA.

Takamura, H., Ebara, S., Hashizume, H., Aizawa, K. & Yamano, H. 2012 Flow visualization and frequency characteristics of velocity fluctuations of complex turbulent flow in a short elbow piping under high Reynolds number condition. *ASME: Journal of Fluids Engineering* **134** (10), 101201.

Tunstall, M. J. & Harvey, J. K. 1968 On the effect of a sharp bend in a fully developed turbulent pipe-flow. *Journal of Fluid Mechanics* **34**, 595–608.

Tunstall, R., Laurence, D., Prosser, R. & Skillen, A. 2016 Large eddy simulation of a T-junction with upstream elbow: The role of Dean vortices in thermal fatigue. *Applied Thermal Engineering* **107**, 672–680.

Wang, Z. & Chung, Y. M. 2016 Direct numerical simulation of a turbulent curved pipe flow. In *11th European Fluid Mechanics Conference*. 12-16 September, Seville, Spain.

Yamano, H., Tanaka, M., Murakami, T., Iwamoto, Y., Yuki, K., Sago, H. & Hayakawa, S. 2011 Unsteady elbow pipe flow to develop a flow-induced vibration evaluation methodology for Japan sodium-cooled fast reactor. *Journal of Nuclear Science and Technology* **48** (4), 677–687.